Mineral mapping by hyperspectral remote sensing in West Greenland using airborne, ship-based and terrestrial platforms

Sara Salehi and Simon Mose Thaarup

While multispectral images have been in regular use since the 1970s, the widespread use of hyperspectral images is a relatively recent trend. This technology comprises remote measurement of specific chemical and physical properties of surface materials through imaging spectroscopy. Regional geological mapping and mineral exploration are among the main applications that may benefit from hyperspectral technology. Minerals and rocks exhibit diagnostic spectral features throughout the electromagnetic spectrum that allow their chemical composition and relative abundance to be mapped.

Most studies using hyperspectral data for geological applications have concerned areas with arid to semi-arid climates, and using airborne data collection. Other studies have investigated terrestrial outcrop sensing and integration with laser scanning 3D models in ranges of up to a few hundred metres, whereas less attention has been paid to ground-based imaging of more distant targets such as mountain ridges, cliffs or the walls of large pits. Here we investigate the potential of using such data in well-exposed Arctic regions with steep topography as part of regional geological mapping field campaigns, and to test how airborne hyperspectral data can be combined with similar data collected on the ground or from moving platforms such as a small ship. The region between the fjords Ikertoq and Kangerlussuaq (Søndre Strømfjord) in West Greenland was selected for a field study in the summer of 2016. This region is located in the southern part of the Palaeoproterozoic Nagssugtoqidian orogen and consists of high-grade metamorphic ortho- and paragneisses and metabasic rocks (see below). A regional airborne hyperspectral data set (i.e. HyMAP) was acquired here in 2002 (Tukiainen & Thorning 2005), comprising 54 flight lines covering an area of *c.* 7500 km^2; 19 of these flight lines were selected for the present study (Fig. 1). The target areas visited in the field were selected on the basis of preliminary interpretations of HyMap scenes and geology (Korstgård 1979).

Two different sensors were utilised to acquire the new hyperspectral data, predominantly a Specim AisaFenix hyperspectral scanner due to its wide spectral range covering the visible to near infrared and shortwave infrared parts of the electromagnetic spectrum. A Rikola Hyperspectral Imager constituted a secondary imaging system. It is much smaller and lighter than the Fenix scanner, but is spectrally limited to the visible near infrared range. The results obtained from combining the airborne hyperspectral data and the Rikola

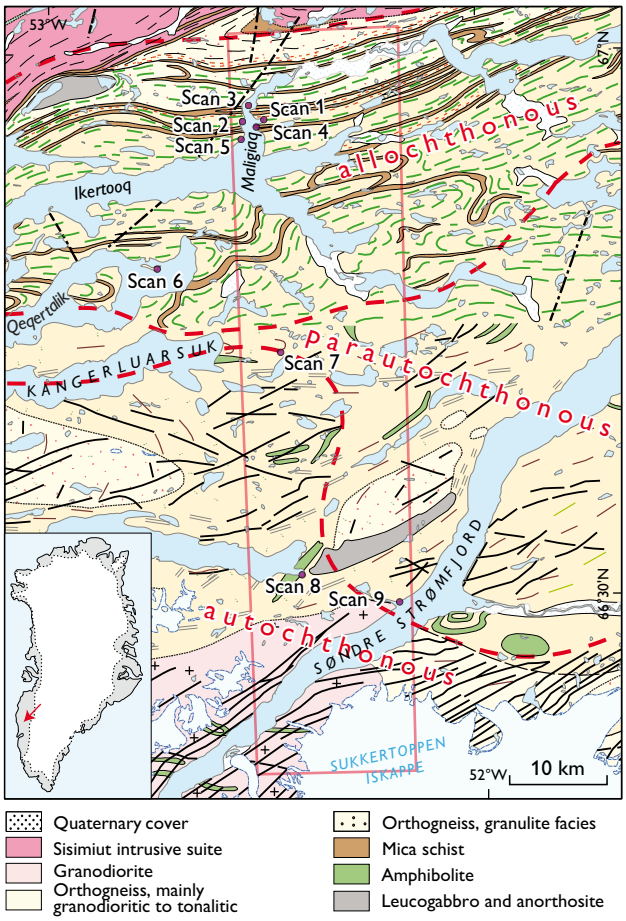

Fig. 1. Geological map across the southern Nagssugtoqidian Orogen simplified from Garde & Marker (2010) and locations of scanned areas mentioned in the text. Red frame: coverage of airborne hyperspectral data selected for this study. From south to north this region comprises (K. Sørensen, personal communication 2018): an autochthonous zone in which deformation regularly increases towards the parautochthonous zone expressed in clockwise rotation of Kangâmiut basic dykes, a parautochthonous zone in which Nagssugtoqidian deformation and metamorphism are highly heterogeneous, and an allochthonous zone where juvenile metasedimentary rocks are interfolded and thrust-stacked with Archaean gneisses containing amphibolitic metadykes.

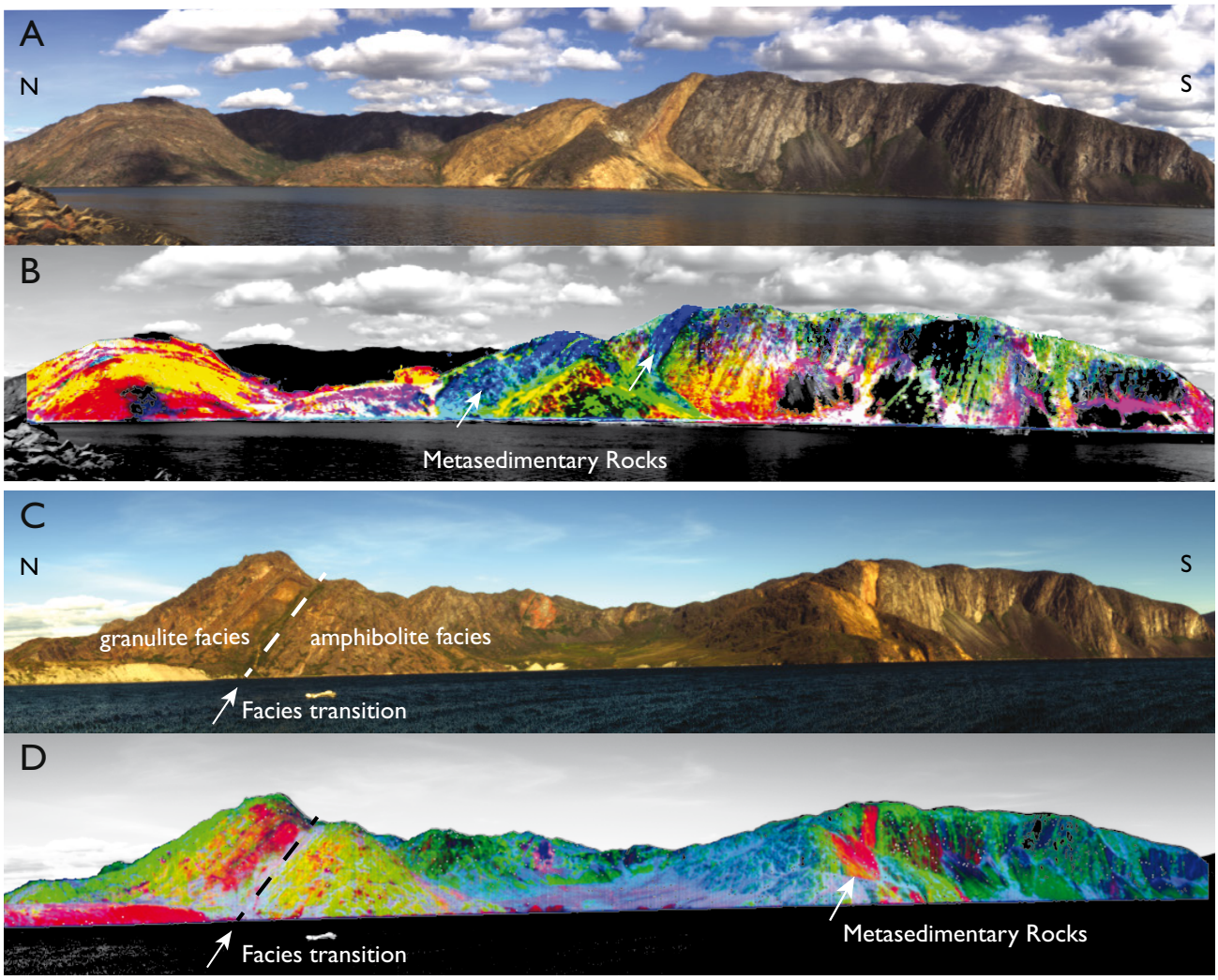

Fig. 2. **A**, **C**: True colour Fenix hyperspectral scenes from the Maligiaq area. See Fig. 1 for scene locations. **B**, **D**: Minimum Noise Fraction false colour image: Red: band 2. Green: band 7. Blue: band 8, overlain on grayscale hyperspectral images.

instrument are presented in Salehi (2018), this volume. In addition, representative samples of the main rock types were collected for subsequent laboratory analysis. A parallel study was integrated with geological and 3D photogrammetric mapping in Karrat region farther north in West Greenland (Rosa *et al.* 2017; Fig. 1).

Analysis of surface mineralogy using sub-horizontal hyperspectral data collection

The extreme influence of atmospheric effects and topography-induced illumination differences in long-range ground-based spectra data cannot be corrected by means of correction tools commonly used for nadir satellite or airborne data. An adapted workflow is presented in Lorenz *et al.* (2018) to overcome the challenges of long-range outcrop sensing, including atmospheric and topographic corrections. Minimum Noise Fraction transformation (Boardman 1993) and Spectral Angle Mapper classification (Kruse *et al.* 1993) were applied to test the applicability of the data for mapping the main rock-forming minerals. The former is important for dimensionality reduction and filtering of noise from hyperspectral data. This method can extract spatially coherent information and show the variations between bands in the hyperspectral data. The Spectral Angle Mapper classification permits rapid mapping of the similarity between image and reference spectra.

Long-range terrestrial hyperspectral scanning in the southern Nagssugtoqidian orogen

In the summer of 2016, new hyperspectral datasets from relatively distant targets were acquired in the allochthonous (Fig. 1, scans 1–6) and autochthonous (Fig. 1, scan 8) zones of the

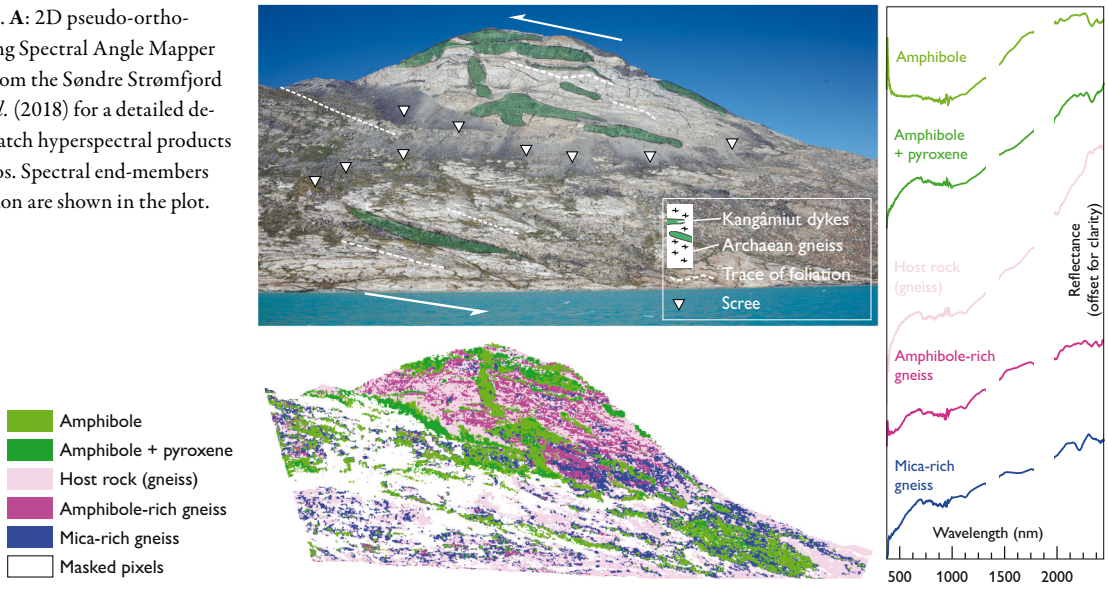

Fig. 3. Scan 9 in Fig. 1. **A**: 2D pseudo-orthophoto. **B**: The resulting Spectral Angle Mapper classification image from the Søndre Strømfjord region. See Salehi *et al.* (2018) for a detailed description of how to match hyperspectral products to pseudo-orthophotos. Spectral end-members used in the classification are shown in the plot.

Nagssugtoqidian orogen. Metasedimentary rocks in the allochthonous zone are tectonically interleaved with quartzofeldspathic gneisses between the southern shore of Qeqertalik fjord and the northern border of the Ikertoq shear zone (Figs 1, 2). Parts of this zone are well exposed along the eastern shore of Maligiaq and were scanned with the Fenix instrument from a distance of *c.* 2–3 km (see Fig. 1 and below). The metasedimentary rocks are predominantly biotite-garnet paragneisses but also comprise aluminous schists and graphitic–sulfidic varieties with up to a few percent graphite and iron sulfides, and they may include both Archaean and Palaeoproterozoic components (see legend to the regional map of Garde & Marker 2010). The scanned area also transects an amphibolite–granulite facies boundary, which follows one of the shear zone branches (Fig. 2). Such facies transitions may be difficult to precisely identify in the field, because the occurrence of the granulite facies index mineral hypersthene depends on bulk rock composition in addition to P, T and xH_2O conditions; hypersthene first occurs in mafic rocks and will be absent from leucocratic metasedimentary and magmatic rocks at similar metamorphic grade. Besides, granulite facies rocks can be retrogressed along younger shear zones.

The result generated from the Fenix spectral data (Fig. 2) highlights the metasedimentary screens. The graphite- and sulphide-bearing schists mapped using such data are shown with purple colour in Fig. 2B and pink in Fig. 2D. The general colour differences are caused by changes in illumination conditions between the acquisition of the two datasets. While graphitic and sulfidic lithologies are readily detected with the Minimum Noise Fraction method used here, the metamorphic transition from amphibolite facies to granulite facies (Korstgård 1979) is not distinguishable; this might be due to absence of diagnostic, hypersthene-bearing lithologies. The boundary might be detected e.g. Matched Filtering (Harsanyi & Chang 1994) and Mixture-tuned Matched Filtering (Boardman 1998), where changes in mineral chemical composition and information on relative abundances of the lithologies are enhanced.

Integration of ship-based hyperspectral scanning and 3D photogrammetry

Mobile mapping of steep coastal cliffs using ship-based hyperspectral scanning was tested – for the first time – in the outer part of the Kangerlussuaq area (Figs 3, 4) and in the related study in the Karrat region mentioned in the introduction. The data processing related to such data acquisition has been fully discussed in Salehi *et al.* (2018).

Our analysis in the former area reveals Kangâmiut dykes intruding intensely deformed Archaean gneisses, besides other metabasic bodies (Fig. 3). The gneissic foliation is clearly identifiable, and several ductile and brittle structures can be observed in the dykes and other metabasic rocks, where amphiboles are the dominant minerals and mica and pyroxene are present with secondary abundances.

The spectral mapping products were integrated with 3D photogrammetric data to create accurate, large-scale outcrop models, which are well suited for quantitative purposes in geological analysis or in preparation for field operations (Fig. 4). For this, a dense and accurate dataset of topographic points (also referred to as a point cloud) can be generated from stereo images describing the terrain surface in three dimensions. The implemented algorithms work reliably even for complex geometries, and with high accuracy. Slightly distorted data, such as images over a low-relief landscape, can be

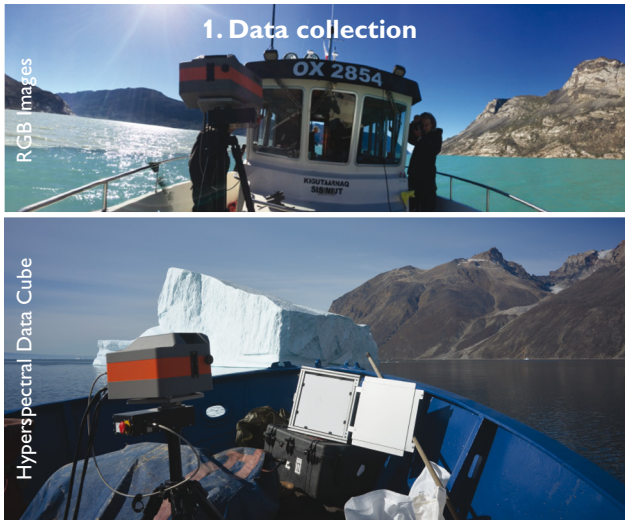

Fig. 4. General workflow for 3D-integration of hyperspectral data cubes and point clouds.

treated quickly using homographic or polynomial transformations, and even data with high local distortions caused by the underlying topography can be processed.

Concluding remarks

The workflow presented here for the acquisition of spectral data from moving platforms and long-range, ground-based hyperspectral scanning opens up a range of new possibilities in the application of hyperspectral imagery by significantly enlarging the scale of measurements. The proposed automatic approach to combine spectral and point cloud data is a fast alternative to manual approaches and has high potential for field geologists who wish to establish accurate outcrop models in areas of difficult access that can be brought to life and visualised in 3D surface models.

Acknowledgments

Kai Sørensen is thanked for constructive discussions on geology. The Helmholtz Institute Freiberg is thanked for the use of the SPECIM AisaFenix hyperspectral scanner and the Rikola Hyperspectral Imager.

References

Boardman, J. 1993: Automated spectral unmixing of AVIRIS data using convex geometry concepts: In: Summaries of the Fourth Annual JPL Airborne Geoscience Workshop October 25–29, 1993. Pasadena, CA: Summaries, JPL Publication 93-26. Vol. 2.

Boardman, J.W. 1998: Leveraging the high dimensionality of AVIRIS data for improved sub-pixel target unmixing and rejection of false positives: mixture tuned matched filtering. In: Summaries of the Seventh Annual JPL Airborne Geoscience Workshop, **97**(1), 55–56.

Garde, A.A. & Marker, M. 2010: Geological Map of Greenland, 1:500 000, Søndre Strømfjord–Nuussuaq, Sheet 1. Second edition. Copenhagen: Geological Survey of Denmark and Greenland.

Harsanyi, J.C. & Chang, C.I. 1994: Hyperspectral image classification and dimensionality reduction: an orthogonal subspace projection approach. IEEE Transactions on geoscience and remote sensing **32**, 779–785.

Korstgård, J.A. 1979: Nagssugtoqidian Geology. Rapport Grønlands geologiske undersøgelse **89**, 63–75.

Kruse, F.A., Lefkoff, A., Boardman, J., Heidebrecht, K., Shapiro, A., Barloon, P. & Goetz, A. 1993: The spectral image processing system (SIPS) – interactive visualization and analysis of imaging spectrometer data. Remote Sensing of Environment **44**, 145–163.

Lorenz, S., Salehi, S., Kirsch, M., Zimmermann, R., Unger, G., Sørensen, E.V. & Gloaguen, R. 2018: Radiometric correction and 3D integration of long-range ground-based hyperspectral imagery for mineral exploration of vertical outcrops. Remote Sensing **10**, 23 pp., *http://dx.doi.org/10.3390/rs10020176*

Rosa, D. *et al.* 2017: Architecture and mineral potential of the Palaeoproterozoic Karrat Group, West Greenland. Results of the 2016 Season. Danmarks og Grønlands Geologiske Undersøgelse Rapport **2017/114**.

Salehi, S. 2018: Hyperspectral analysis of lithologies in the Arctic in the presence of abundant lichens. Geological Survey of Denmark and Greenland Bulletin **41**, 51–55 (this volume).

Salehi, S., Lorenz, S., Sørensen, E.V., Zimmermann, R., Fensholt, R., Heincke, B.H., Kirsch, M. & Gloaguen, R. 2018: Integration of vessel-based hyperspectral scanning and 3D-photogrammetry for mobile mapping of steep coastal cliffs in the Arctic. Remote Sensing **10**, 26 pp, *http://dx.doi.org/10.3390/rs10020175*

Tukiainen, T. & Thorning, L. 2005: Detection of kimberlitic rocks in West Greenland using airborne hyperspectral data: the HyperGreen 2002 project. Geological Survey of Denmark and Greenland Bulletin **7**, 69–72.

Authors' address

S.S. & S.M.T., *Geological Survey of Denmark and Greenland, Øster Voldgade 10, DK-1350 Copenhagen K, Denmark.* E-mail: *ssal@geus.dk.*